JOURNAL OF MACROMOLECULAR SCIENCE®
Part B—Physics
Vol. 42, No. 2, pp. 387–401, 2003

Primary Crystal Nucleation and Growth Regime Transition in Isotactic Polypropylene

Annamaria Celli,* Edgar D. Zanotto, and Isak Avramov#

Vitreous Materials Laboratory—LaMaV, Department of Materials Engineering—DEMa, Federal University of São Carlos—Ufscar, São Carlos-SP, Brazil

ABSTRACT

We studied nucleation and crystal growth in two polypropylene samples by analyzing the number of spherulites, their size, and shape for various treatments in a hot-stage microscope. The consistency of nucleation and growth data were tested by using overall crystallization experiments and the Jonhson–Mehl–Avrami–Kolmogorov equation. In isothermal conditions, for temperatures, T_C, varying between 123° and 138°C, the number of crystallites per unit area does not depend on crystallization time and temperature. Instead, at small undercoolings (for $T_C > 138$°C), the total number of nuclei per unit area remains independent of crystallization time, but decreases with increasing temperature. We discuss the implications of this finding for the final microstructure of the crystallized samples. It is noteworthy that the passage between these two nucleation behaviors coincides with the transition from regime III to regime II, observed in the crystal growth kinetic analysis. This remarkable correlation between primary nucleation and crystal growth regimes is discussed.

Key Words: Primary nucleation; Crystal growth; Regime transition; Crystallization; Isotactic polypropylene.

*Correspondence: Annamaria Celli, Department of Applied Chemistry and Materials Science, University of Bologna, Viale Risorgimento 2, 40136 Bologna, Italy; E-mail: annamaria.celli@mail.ing.unibo.it.

#Current address: Institute of Physical Chemistry, Bulg. Acad. Sci., 1113 Sofia, Bulgaria.

DOI: 10.1081/MB-120017126 0022-2348 (Print); 1525-609X (Online)

INTRODUCTION

Crystallization controls the final microstructure and, consequently, the properties and applications of semicrystalline polymers. Although crystal growth and overall crystallization kinetics of a plethora of polymers have been extensively analyzed, nucleation studies are rare. The reason for the paucity of nucleation studies is the difficulty in obtaining reliable experimental data through the most common thermal analysis techniques. In fact, nucleation occurring in viscous liquids, cooled from the melting point, cannot be detected by differential scanning calorimetry (DSC) due to the small quantity of heat involved, and cannot be directly observed by optical microscopy because of the small size of the nuclei. Moreover, measurements of hot-stage light depolarization (HSLD) microscopy do not reveal the first stages of crystallization. Owing to the low sensitivity of these experimental techniques, results obtained by thermal analyses may be erroneously evaluated. Only recently have a few studies on nucleation been carried out using other experimental approaches [e.g., by small- and wide-angle X-ray scattering (SAXS and WAXS)],[1–3] atomic force microscopy,[4] small-angle light scattering,[5] and coupled SAXS and FTIR analyses.[6] On the other hand, in view of the difficulties involved in obtaining significant experimental data, theoretical evaluations of nucleation, based on thermodynamic and kinetic considerations, have also been reported.[7]

In this article, a large effort has been made to obtain significant quantitative data of the nucleation process by using a classical thermal analysis technique—hot-stage optical microscopy—and by carefully observing the effects of nucleation on the resulting microstructures, in particular on the number, size, and shape of spherulites. These data were completed by crystal growth measurements and overall crystallization studies with light depolarization microscopy and DSC analyses. The first objective of this article is to verify the consistency of the nucleation and growth data obtained by the classical thermal analysis techniques. After this important test, meaningful nucleation and growth rate data were available to study the primary and secondary nucleation processes and their possible connections. For the first time, a remarkable correlation between primary nucleation and the well-known crystallization regimes proposed by Hoffman et al.[8] was observed. If confirmed in other polymers, this result should be particularly interesting for the comprehension of crystallization processes in macromolecules.

EXPERIMENTAL

Two isotactic polypropylene (PP) homopolymers[9] produced by Montell (Ferrara, Italy) were analyzed. Specimen A is characterized by intrinsic viscosity $[\eta] = 3.48\,\mathrm{dL\,g^{-1}}$, $M_w = 947,000$, $M_w/M_n = 8.7$, and isotactic index = 96.5%, determined by nuclear magnetic resonance triads. Sample B is characterized by $[\eta] = 0.66\,\mathrm{dL\,g^{-1}}$, $M_w = 129,000$, $M_w/M_n = 11$, and isotactic index = 97%. The addition of 1,600 ppm per weight of a mixture of Irganox 1010 and Irgafos 168 stabilized the specimens in a 1:2 ratio.

Crystallization studies were performed under nitrogen flux in a Leitz polarizing microscope (Labor Lux S) equipped with a Linkam TMHS 600 hot-stage camera and video camera. This experimental apparatus will be designated HSG in the following

sections. The calibration of the hot stage was checked by common standards at a heating rate of 2°C/min. The reproducibility and stability of the hot stage were verified by comparing the kinetic results of different growth cycles.

Cast films, 20 μm thick, were obtained from solutions of PP in *o*-xylene. The films were heated at 10°C/min to the temperature $T_F = 200$°C, above the equilibrium melting point, kept at this temperature for 5 min, cooled at ~80°C/min to the selected crystallization temperature, T_C, and kept at T_C for sufficiently long times for significant crystallization. This thermal treatment is represented in Fig. 1. The fast cooling from T_F to T_C was obtained by a cold nitrogen flux inside the hot stage: the effective rate, at which the sample reaches T_C, slightly varied for each experiment depending on the undercooling. The 80°C/min represents a good compromise between the highest attainable cooling rate and the absence of overshooting, as verified by a thermocouple inserted inside the hot-stage apparatus. The T_C range analyzed varied from 123° to 150°C for both samples. At these crystallization temperatures, the slow rate of crystallization allows one to easily follow the spherulitic growth. At each T_C, numerous micrographs were taken at different times (t_C), whereas the sample was crystallizing, and the average numbers of spherulites per unit area were counted as a function of t_C. The number of spherulites was assumed to correspond to the number of stable nuclei per unit area (N_S) grown in the melt. The spherulitic radii (r) were measured with a grilled system in the video before crystal impingement. The growth rate (G) was calculated from the slope of the straight line obtained from r vs. t_C plots.

Overall, crystallization experiments were performed by HSLD and DSC. The evolution of crystallization was followed by continuous measurements of the light depolarization signal as a function of time. Measurements were carried out in an Orthoplan polarizing microscope, equipped with a Mettler FP52 heating device, coupled with a photosensitive diode in the eyepiece. Crystallization experiments of bulk specimens were conducted under nitrogen flux in a Perkin–Elmer DSC-7 instrument, using 10–20 mg of *iso*-PP. The temperature scale of DSC was calibrated with high purity standards. For both

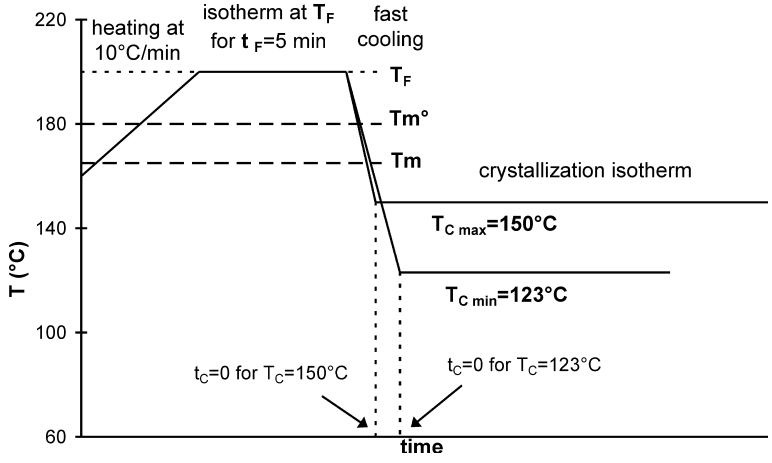

Figure 1. Scheme of the thermal treatments in HSG for samples A and B.

HSLD and DSC, the experimental procedure consisted of melting at 200°C for 5 min, fast cooling at 80°C/min to T_C, isothermal crystallization at T_C, followed by reheating from T_C to 200°C at 10°C/min. The T_C range over which data could be collected was limited to 120–135°C, due to the instrument's sensitivity. In fact, at T_C below 120°C, it was not possible to obtain a stable signal output before changes in light depolarization signal and in heat flow, owing to the rapid crystallization. At T_C above 135°C, crystallization was too slow to obtain a significant variation of the baseline. The equilibrium melting temperatures (T_m°) were determined by extrapolation of the melting temperatures, measured in DSC thermograms, with respect to the crystallization temperatures T_C, according to the Hoffman–Weeks procedure.[10] It is reported that significant T_m° data are obtained if the lamellar thickness is small, defined, and maintained at each T_C, and that these conditions can be verified if the slope of the T_m vs. T_C plot is equal to 0.5.[11] Then, the crystallization conditions, used to determine T_m°, were adequately chosen, mainly in terms of short crystallization times, to obtain a T_m vs. T_C slope very close to 0.5. The resulting T_m° values are 184.5°C for PP-A and 178.9°C for PP-B. The reported T_m° of *iso*-PP are somewhat uncertain: the values of T_m° obtained by extrapolation of $T_m = f(T_C)$ curves fall into two groups, one around 186°C and the other around 210°C, and strongly depend on the T_C range analyzed. Mezghani et al.[12] discuss about this uncertainty in terms of lamellar thickening occurring during the isothermal crystallization: by combined SAXS, DSC, and HSLD measurements, they determine a T_m° value for *iso*-PP close to 186°C. Also, other papers that are focused on the study of the transition regimes in *iso*-PP report similar results.[13,14] Therefore, the T_m° values obtained for samples A and B agree with significant literature data.

Wide-angle X-ray scattering analysis was performed on samples isothermally crystallized in DSC and then fast-cooled to room temperature. The PP α-phase was the polymorphic form crystallized in the T_C range analyzed for both samples.

RESULTS AND DISCUSSION

Crystal Nucleation

The nucleation process was studied by observing the crystallization under isothermal conditions using HSG equipment. In both samples A and B and in all the crystallization experiments, some small circular particles grow as α-spherulites. By counting them in photographs taken at different t_C, their number remains constant from their appearance to full growth. Then, the nucleation process in both samples shows no time dependence and occurs from a limited number of pre-existing sites on the sample surfaces, as observed for many polymers, including *iso*-PP (e.g., Refs.[15–18]). The predetermined nuclei present in the melt can be either heterogeneous sites, formed by foreign particles, such as catalysts, additives, or impurities, or athermal nuclei, due to crystal fragments left from uncompleted melting. In this latter case, the number of nuclei is strictly dependent on the thermal history.[19–21] It has been reported that only at very large undercoolings, for T_C lower than 80°C, homogeneous nucleation becomes predominant in *iso*-PP.[22]

From the micrographs, it was possible to count the number of spherulites per unit area (N_S) characteristic of each T_C. These values are reported in Table 1, with

Table 1. Average number of nuclei per unit area (N_S) obtained during isothermal crystallization at T_C and at undercooling $\Delta T = T_m^\circ - T_C$, for PP-A and PP-B.

	Sample A		Sample B	
T_C (°C)	ΔT	N_S (cm^{-2})	ΔT	N_S (cm^{-2})
125	59.5	3.51E4	53.9	2.90E3
128	56.5	3.70E4	50.9	3.80E3
130	54.5	3.54E4	48.9	5.00E3
132	52.5	3.65E4	46.9	2.90E3
135	49.5	3.55E4	43.9	2.10E3
138	46.5	3.49E4	40.9	5.00E3
140	44.5	2.80E4	38.9	3.80E3
142	42.5	2.00E4	36.9	3.20E3
145	39.5	1.82E4	33.9	8.00E2
148	36.5	1.05E4	30.9	2.00E2
150	34.5	1.23E4	28.9	4.00E2

the corresponding undercooling ($\Delta T = T_m^\circ - T_C$) for the two samples. It is evident that, at similar undercooling, N_S is always higher for sample A than for sample B. This behavior can be attributed either to a difference in the number of heterogeneous nuclei[23] or to the presence of more numerous athermal nuclei in sample A. In fact, for sample A, characterized by a higher T_m°, the melting conditions used (T_F and t_F) were softer, and thus more important melting memory effects could occur.[19,20,24]

F2 The dependence of N_S on T_C for samples A and B is reported in Fig. 2. It is worth noting that the number of nuclei is nearly constant in the T_C range from 125° to 138°C for both samples A and B. For PP-A, N_S fluctuates around $(3.60 \pm 0.15) \times 10^4$ nuclei/cm^2, whereas for PP-B, it fluctuates around $(0.35 \pm 0.15) \times 10^4$ nuclei/cm^2. In contrast, at higher T_C (from 138° to 150°C), N_S decreases as the crystallization temperature increases: for PP-A to about 1.1×10^4 nuclei/cm^2, for PP-B to 4×10^2 nuclei/cm^2.

F3 Figure 3a and b shows the growth curves [radius (r) vs. time (t_C)] for some crystallization temperatures above and below 138°C, respectively, for both polymers. For each T_C, the data, referring to two or three different spherulites, grown under the same conditions, can be extrapolated by only one straight line. This behavior indicates that, at each T_C, the linear growth rate (G) is a constant and confirms that the time at which spherulites appear in the melt is always the same. This result agrees with experimental evidence reported in the literature on the formation of a crystalline order (e.g., a mesomorphic phase[2]) before crystal growth. The intercepts of the extrapolated lines, drawn in Fig. 3a and b, calculated for $r = 0$, give the induction time values (τ). For $T_C \leq 138$°C (Fig. 3a), the values of τ are always negative, whereas for $T_C > 138$°C (Fig. 3b), τ is always positive. In the latter case, τ increases as T_C increases. It is important to emphasize that these data are quite reproducible.

As thin ($\sim 20\,\mu$m) films of *iso*-PP were used, it is possible to assume that the samples reach T_C at the same time as the instrument, with no appreciable thermal lag. Therefore, a negative τ indicates that nucleation takes place on the (fast) cooling path from T_F to T_C.

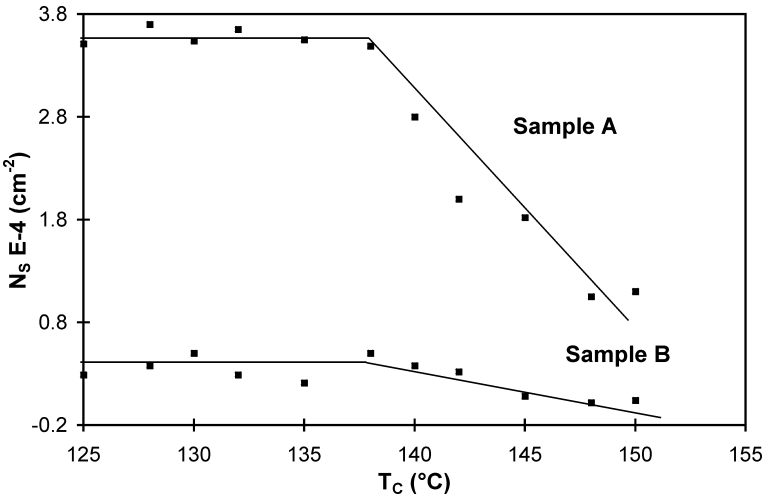

Figure 2. Average number of nuclei per unit area (N_S) as a function of crystallization temperature for samples A and B.

A positive τ, in contrast, corresponds to a nucleation process that takes place at T_C. Then, the N_S vs. T_C trend of Fig. 2 can be explained by assuming that, at T_C lower than 138°C (left part of Fig. 2), the real nucleation temperature is always the same, independent of T_C, and is located between T_F and T_C. This nucleation temperature is related with the exhaustion of the nucleation sites present in the melt. As a consequence, the N_S value does not depend on T_C. At T_C higher than 138°C (right part of Fig. 2), instead, the nucleation temperature really corresponds to the temperature of isothermal hold. Then, as the critical nucleus size increases with T_C, not all the heterogeneous sites can originate a spherulite: this is the reason why it seems that part of the active nucleating centers are deactivated by rising temperatures.

This nucleation behavior has important consequences on material's microstructure. At low T_C (<138°C), the final microstructure does not change by modifying the crystallization conditions: the micrographs always show the presence of a large number of small spherulites covering the entire sample surface. At high T_C (>138°C), instead, the number of spherulites decreases with increasing T_C and, then, the average spherulite radius increases, reaching quite large dimensions.

Consistency Analysis

In most papers dealing with polymer crystallization, only nucleation, growth, or overall crystallization kinetics are measured.[25–31] In addition, indirect techniques are frequently used. The reliability of such kinetic data is thus often subject to uncertainty. In this article, instead, we measure the three significant quantities (nucleation, growth, and overall crystallization) and test their consistency.

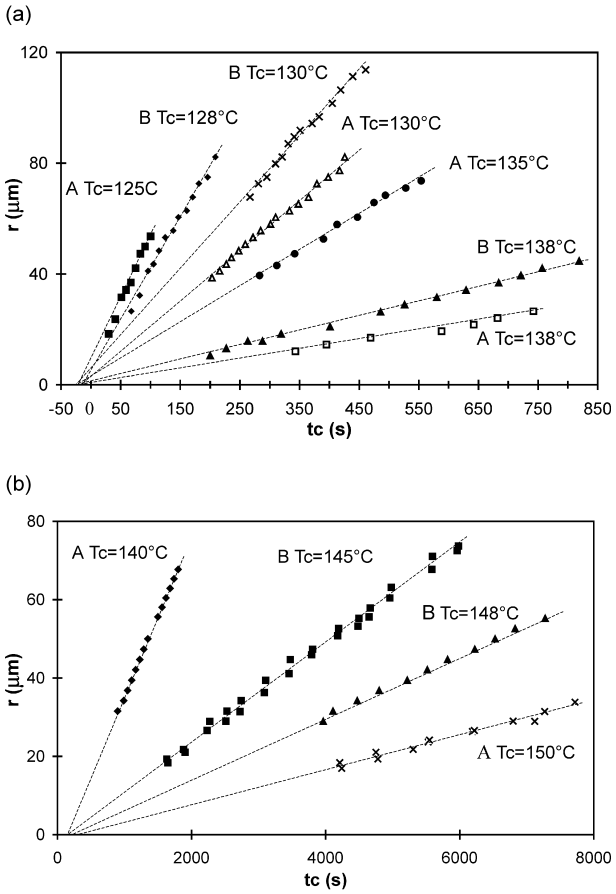

Figure 3. Spherulite radius (r) vs. crystallization time (t_C) for both polymers: (a) $T_C \leq 138$°C and (b) $T_C > 138$°C.

The significance of the N_S and G data, obtained by HSG and reported in Table 1, can be verified by using a method based on the overall crystallization measurements carried out by HSLD and DSC. Data are analyzed by using the Jonhson–Mehl–Avrami–Kolmogorov (JMAK) equations[28–31]:

$$X = 1 - \exp(-Kt^n) \tag{1}$$

where X is the fraction crystallized under isothermal conditions, and K is a kinetic constant, which combines both nucleation and growth rates; t is the time; and n is a constant that depends on the dimensionality of crystal growth and on the nucleation mechanism. For overall crystallization experiments performed both in HSLD and in DSC, for samples A and B and for all the temperatures studied, the values of n result indeed at about 2. In particular $n = 1.9 \pm 0.1$ for polymer B and $n = 1.8 \pm 0.1$ for polymer A. Recalling that, for a constant number of growing crystals per unit surface, N_S, and for

Table 2. Growth rate (G), measured by HSG, semicrystallization time ($t_{1/2}$), measured by DSC, and crystalline fraction (X_C), measured by WAXS, for PP-A and PP-B samples crystallized at different T_C.

	Sample A				Sample B			
T_C (°C)	ΔT	G (μm/sec)	$t_{1/2}$ (sec)	X_C (%)	ΔT	G (μm/sec)	$t_{1/2}$ (sec)	X_C (%)
120	64.5	—	91	58	58.9	—	56	67
123	61.5	0.550	161	59	55.9	1.037	100	79
125	59.5	0.500	242	48	53.9	0.635	165	62
128	56.5	0.260	427	57	50.9	0.368	251	65
130	54.5	0.183	825	64	48.9	0.238	599	51
132	52.5	—	1870	65	46.9	0.151	1271	74
135	49.5	0.090	3310	61	43.9	0.080	1789	70
138	46.5	0.048	—	—	40.9	0.040	—	—
140	44.5	0.040	—	—	38.9	0.036	—	—
142	42.5	0.035	—	—	36.9	0.022	—	—
145	39.5	0.025	—	—	33.9	0.013	—	—
148	36.5	—	—	—	30.9	0.008	—	—
150	34.5	0.011	—	—	28.9	0.005	—	—

time-independent growth rate (G), K can be expressed by:

$$K = \pi G^n N_S \tag{2}$$

we build theoretical curves $X = f(t)$, combining Eqs. (1) and (2). The value of n is fixed equal to 2, the G data reported in Table 2 are used, and the N_S value is varied. The best fit between these theoretical curves and the experimental data obtained by HSLD is observed when N_S values are included within the experimental limits (Table 1). For example, Fig. 4 illustrates the overall crystallization data for sample B at two crystallization temperatures: solid lines are drawn according to Eqs. (1) and (2). The good agreement observed suggests that, for samples A and B, the most probable N_S values coincide, within experimental accuracy, with the data obtained by the direct observation of crystallization in HGS. This method, based on the use of the JMAK equation, provides an important confirmation of the consistency of the experimental nucleation and growth data that, in turn, allows us to analyze further if there is any relationship between these kinetic quantities.

Crystal Growth Process

Growth rates (G) are reported in Fig. 5 as a function of ΔT. It is evident that, at the same undercooling, for $\Delta T > 40$, sample B is characterized by a higher growth rate than sample A, showing the expected effect of molecular weight on growth kinetics. This result is confirmed by the data of the semicrystallization time ($t_{1/2}$) [i.e., the time necessary to reach 50% of total crystallinity, obtained by studying the overall crystallization process by DSC (see Table 2)]. Concerning the degree of crystallinity reached after "complete" crystallization, the X-ray diffraction analysis indicates that X_C varies little with T_C, as

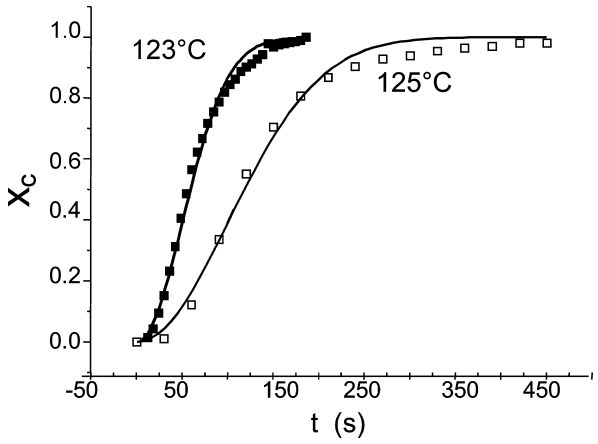

Figure 4. Overall crystallization kinetics for sample B annealed at 123°C and 125°C. Solid lines are drawn according to Eqs. (1) and (2), with $n = 2$, $G =$ experimentally determined, and $N_S =$ best fit. The fitted values lie within the experimental limits [i.e., $(3.5 \pm 0.15) \times 10^4$ nuclei/cm^2].

confirmed by Cheng et al.[14] in the range of ΔT analyzed, and decreases with increasing molecular weight, as generally expected.[32,33]

The kinetics of crystal growth in polymers are often analyzed by the Hoffman–Lauritzen equation[8]:

$$G(T) = G_o \exp[-U^*/(R(T_C - T_\infty))] \exp[-K_g/(fT_C\Delta T)] \tag{3}$$

where G_o is a pre-exponential factor containing quantities that are not strongly dependent on temperature; $U*$ is a "universal" constant, characteristic of the activation energy for

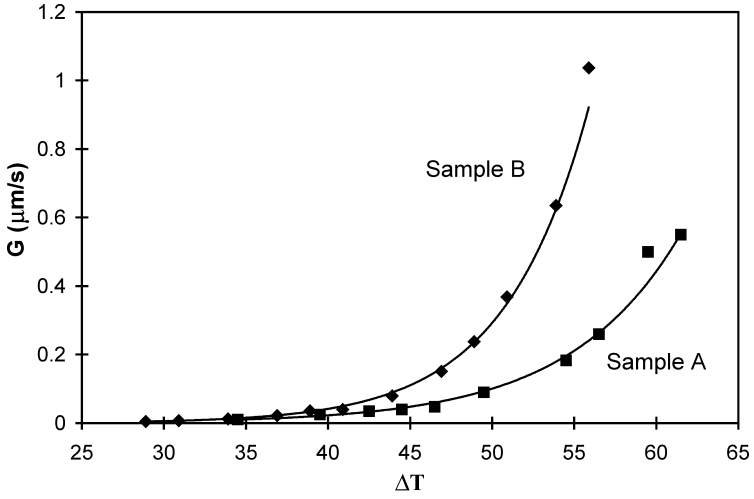

Figure 5. Growth rate (G) as a function of undercooling (ΔT) for samples A and B.

reptation in the melt, which is typically taken as 6,280 J/mol, e.g. Ref.[8]; R is the gas constant; and T_∞ represents the theoretical temperature below which all motion associated with viscous flow or reptation ceases. T_∞ is usually assumed to be equal to ($T_g - 30$°C). The term $f = 2T_C/(T_C + T_m^\circ)$ is a correction factor introduced to account for the temperature dependence of the heat of crystallization. The (secondary) nucleation constant K_g, which controls crystal growth, is expressed by:

$$Kg_{\mathrm{III}} = Kg_{\mathrm{I}} = 4b_\infty \sigma\sigma_e T_m^\circ/(\Delta H_m k) \quad \text{in regimes III and I}$$

and by

$$Kg_{\mathrm{II}} = 2b_o \sigma\sigma_e T_m^\circ/(\Delta H_m k) \quad \text{in regime II}$$

b_o is the thickness of a single stem on the crystal, σ and σ_e are the lateral and fold surface-free energies, respectively, and k is the Boltzmann constant.

F6 Figure 6 represents a linearized form of Eq. (3) [i.e., the relationship between $\ln(G) + U^*/(R(T_C - T_\infty))$ and $1/(fT_C\Delta T)$. For both samples, a transition from regime III to regime II occurs at a temperature close to 138°C, corresponding to an undercooling $\Delta T = 47$°C for sample A and 41°C for sample B. These results are similar to those of Clark et al.[34] and Janimak et al.,[35] who describe a regime transition from III to II at an undercooling $\Delta T = 48$°C, for PP fractions of different isotacticity. For each sample, the two nucleation constants Kg_{III} and Kg_{II} are calculated by the slopes of the straight lines of Fig. 6 and their ratio $Kg_{\mathrm{III}}/Kg_{\mathrm{II}}$ is equal to 2, as predicted by theory.[8] It is noteworthy that the growth regime transition occurs at the same temperature (~138°C) at which the nucleation behavior changes and the number of nuclei switches from a constant value to a temperature-dependent one (Fig. 2). Therefore, correlation between primary nucleation behavior and growth regime transition seems to exist. The most evident effect of this correlation is given by observing the final morphology: in regime III, *iso*-PP samples are characterized by a very high number of small spherulites, that remains constant, independent of T_C. In regime II, instead, the number of spherulites decreases and, correspondingly, their size increases by increasing T_C. To the best of our knowledge, such

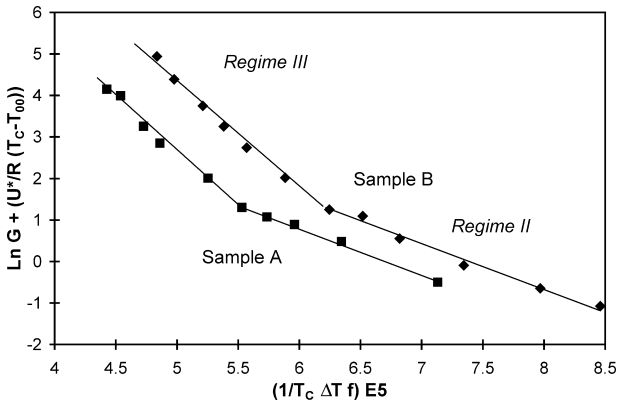

Figure 6. Crystallization regimes III and II for samples A and B.

correlation has never been reported in the literature and may be just a coincidence, but it clearly occurs for both polymers. Hence it deserves further attention.

Numerous papers deal with the problem of finding comprehension of the regime transitions by correlating them with some physical, morphological, or structural change. In particular, many authors have tried to interpret the change of crystallization regimes by morphological modifications.[36–42] Indeed, morphological changes are present in samples A and B only in terms of spherulites number. On the other hand, correlations between crystal growth kinetics and primary nucleation are not frequently found. Hoffman[36] discusses the possibility that melting memory effects and, then, primary crystallization, influence crystallization kinetics; but, he concludes that these effects do not invalidate the secondary nucleation (that controls crystal growth) theory based on crystallization regimes.

It is possible to discuss primary and secondary nucleation in the same terms: the formation of a primary nucleus that originates as a spherulite, and the deposit of a secondary nucleus that causes lamella growth have a common key factor based on the dependence of the critical nucleus size on temperature. From experimental results, it is evident that, at T_C lower than 138°C, nucleation centers existing in the melt (N_S per unit area) seem to be all active to initiate crystallization. At the same time, in the crystal growth occurring in regime III, steams are easily deposited on the lamellae, including the tiniest seeds having a size of the order of the lamellae thickness.

On the other hand, above 138°C, as the critical nucleus size increases with the temperature, the submicroscopic foreign seeds can act as nucleation catalysts only if they are at least as large as the critical nucleus. The number of seeds that do not satisfy this condition and that will become inactive, will increase with temperature (as seen in Fig. 2, where N_S decreases with T_C). Correspondingly, during growth that occurs in regime II, a significant barrier for attachment of first steam is present.[8,36] Therefore, part of the seeds is deactivated and the dependence of the growth rate with temperature has a break (shown in Fig. 6). Then, the coincident behavior between primary and secondary nucleation can be expressed in terms of substrate activity as a function of temperature.

CONCLUSIONS

Although numerous papers study nucleation, crystal growth, or overall crystallization of *iso*-PP, complete and simultaneous analyses of nucleation, growth, and overall crystallization on the same samples—in the same temperature range—are quite rare. Such experimental approach, if carefully performed, can give interesting information about the thermal behavior of polymers.

In the present article, the results of a detailed study on the evolution of average number, size, and shape of spherulites and on overall crystallization rate are reported and discussed. It is noteworthy that all the thermal data, even those obtained by different experimental techniques, are consistent, as tested by the JMAK equation.

The dependence of the nuclei number on the crystallization temperature and time shows that athermal heterogeneous nucleation is predominant in *iso*-PP. Moreover, it is significant that at large undercoolings, for $T_C < 138$°C, the number of crystallites does not depend on time or annealing temperature. At small undercoolings, on the other hand, for

$T_C > 138$°C, the number of spherulites does not depend on time, but decreases with increasing temperature.

Surprisingly, this change in nucleation behavior at 138°C coincides with the growth regime transition III → II. Consequently, in regime III, a constant (high) number of small spherulites is present, independent of temperature, whereas in regime II, the number of spherulites decreases and their size increases as temperature increases. This remarkable correlation observed between nucleation and growth behavior has been interpreted as due to the substrate activity as a function of temperature.

To the best of our knowledge, this coincident behavior between primary and secondary nucleation has never been reported in the literature: in general, the relationship between crystal growth regimes and microstructural features was not discussed in terms of primary nucleation behavior. However, the results observed for *iso*-PP-A and *iso*-PP-B may be coincidental. Thus, further studies, with other polymers, will be necessary to generalize or not the present finding. If confirmed, there will be scope to improve the understanding of the correlation existing between primary and secondary crystallization.

NOMENCLATURE

DSC	differential scanning calorimetry
HSG	hot-stage microscopy equipped with camera and videocamera for G determination
HSLD	hot-stage light depolarization
JMAK	Jonhson–Mehl–Avrami–Kolmogorov
PP	polypropylene
SAXS	small-angle X-ray scattering
WAXS	wide-angle X-ray scattering
T_m	melting temperature of the sample
T_m°	equilibrium melting temperature
T_F	temperature at which the polymers are melted in HSG, HSLD, and DSC
t_F	time of isotherm at T_F
T_C	isothermal crystallization temperature
t_C	isothermal crystallization time
ΔT	$(T_m^\circ - T_C)$, undercooling
G	spherulitic growth rate
r	spherulitic radius
N_S	average number of nuclei per unit area
X_C	crystalline fraction measured by WAXS

REFERENCES

1. Terrill, N.J.; Fairclough, P.A.; Towns-Andrews, E.; Komanschek, B.U.; Young, R.J.; Ryan, A.J. Density fluctuations: the nucleation event in isotactic polypropylene crystallization. Polymer **1998**, *39*, 2381–2385.

2. Wang, Z.-G.; Hsiao, B.S.; Srinivas, S.; Brown, G.M.; Tsou, A.H.; Cheng, S.Z.D.; Stein, R.S. Phase transformation in quenched mesomorphic isotactic polypropylene. Polymer **2001**, *42*, 7561–7566.
3. Iijima, M.; Strobl, G. Isothermal crystallization and melting of isotactic polypropylene analyzed by time- and temperature-dependent small-angle x-ray scattering experiments. Macromolecules **2000**, *33*, 5204–5214.
4. Li, L.; Chan, C.-M.; Li, J.-X.; Ng, K.-M.; Yeung, K.-L.; Weng, L.-T. A direct observation of the formation of nuclei and the development of lamellae in polymer spherulites. Macromolecules **1999**, *32*, 8240–8242.
5. Pogodina, N.V.; Siddiquee, S.K.; van Egmond, J.W.; Winter, H.H. Correlation of rheology and light scattering in isotactic polypropylene during early stages of crystallization. Macromolecules **1999**, *32*, 1167–1174.
6. Sasaki, S.; Tashiro, K.; Kobayashi, M.; Izumi, Y.; Kobayashi, K. Microscopically viewed structural change of PE during the isothermal crystallization from the melt II. Conformational ordering and lamellar formation mechanism derived from the coupled interpretation of time-resolved SAXS and FTIR data. Polymer **1999**, *40*, 7125–7135.
7. Janeschitz-Kriegl, H. Conditions of nucleation in crystallizable polymers: reconnaissance of positions—a critical evaluation. Colloid Polym. Sci. **1997**, *275*, 1121–1135.
8. Hoffman, J.D.; Davis, G.T.; Lauritzen, J.I., Jr. *Treatise on Solid-State Chemistry*; Plenum Press: New York, 1976; Vol. 3, Chap 7.
9. Celli, A.; Zanotto, E.D. Polymer crystallization: fold surface free energy determination by different thermal analysis techniques. Thermochim. Acta **1995**, *269/270*, 191–199.
10. Hoffman, J.D.; Weeks, J.J. J. Res. Natl. Bur. Stand. (A) **1962**, *66*, 13.
11. Mandelkern, L. Crystallization and melting. *Comprehensive Polymer Science*; Pergamon Press: Oxford, 1989; Vol. 2.
12. Mezghani, K.; Campbell, A.R.; Phillips, P.J. Lamellar thickening and the equilibrium melting point of polypropylene. Macromolecules **1994**, *27*, 997–1002.
13. Cheng, S.Z.D.; Janimak, J.J.; Zhang, A.; Cheng, H.N. Regime transitions in fractions of isotactic polypropylene. Macromolecules **1990**, *23*, 298–303.
14. Cheng, S.Z.D.; Janimak, J.J.; Zhang, A.; Hsieh, E.T. Isotacticity effect on crystallization and melting in polypropylene fractions: 1. Crystalline structures and thermodynamic property changes. Polymer **1991**, *32*, 648–655.
15. Binsbergen, F.L. Natural and artificial heterogeneous nucleation in polymer crystallization. J. Polym. Sci.: Polym. Symp. **1977**, *59*, 11–29.
16. Price, F.P. *Nucleation*; Zettlemoyer, A.C., Ed.; Marcel Dekker: New York, 1969; Chap. 8.
17. Sharples, A. *Introduction to Polymer Crystallization*; Edward Amold Ltd: London, 1965.
18. Wunderlich, B. *Macromolecular Physics, Vol. 2, Crystal Nucleation, Growth, Annealing*; Academic: New York, 1976; .
19. Ziabicki, A.; Alfonso, G.C. Memory effects in isothermal crystallization I. Theory. Colloid Polym. Sci. **1994**, *272*, 1027–1042.

20. Alfonso, G.C.; Ziabicki, A. Memory effects in isothermal crystallization II. Isotactic polypropylene. Colloid Polym. Sci. **1995**, *273*, 317–323.
21. Janeschitz-Kriegl, H.; Ratajski, E.; Wippel, H. The physics of athermal nuclei in polymer crystallization. Colloid Polym. Sci. **1999**, *277*, 217–226.
22. Bartczak, Z.; Galeski, A. Homogeneous nucleation in polypropylene and its blends by small-angle light scattering. Polymer **1990**, *31*, 2027–2038.
23. Deslandes, Y.; Sabir, F.-N.; Roovers, J. Effect of molecular weight on the spherulitic growth rate of poly(aryl ether ether ketone). Polymer **1991**, *32*, 1267–1273.
24. Varga, J. Supermolecular structure of isotactic polypropylene. J. Mater. Sci. **1992**, *27*, 2557–2579.
25. Bicerano, J. Crystallization of polypropylene and poly(ethylene terephthalate). J.M.S. Rev. Macromol. Chem. Phys. **1998**, *C38*, 391–479.
26. Bartzack, Z.; Galeski, A.; Pracella, M. Spherulite nucleation in blends of isotactic polypropylene with high-density polyethylene. Polymer **1986**, *27*, 537–543.
27. Galeski, A. *Polypropylene Structure, Blends and Composites*; Chapman & Hall: London, 1995; Vol. 1, Chap. 4.
28. Galeski, A.; Bartczak, Z.; Pracella, M. Spherulite nucleation in polypropylene blends with low density polyethylene. Polymer **1984**, *25*, 1323–1326.
29. von Falkai, B. Schmelz- und Kristallisationserscheinungen bei makromolekularen substanzen. Makromol. Chem. **1960**, *41*, 86–109.
30. Binsbergen, F.L.; De Lange, B.G.M. Heterogeneous nucleation in the crystallization of polyolefins: part 2. Kinetics of crystallization of nucleated polypropylene. Polymer **1970**, *11*, 309–332.
31. Menczel, J.; Varga, J. Influence of nucleating agent on crystallization of polypropylene I. Talc as nucleating agent. J. Therm. Anal. **1983**, *28*, 161–174.
32. Day, M.; Deslandes, Y.; Roovers, J.; Suprunchuk, T. Effect of molecular weight on the spherulitic growth rate of poly(aryl ether ether ketone): a differential scanning calorimetry study. Polymer **1991**, *32*, 1258–1266.
33. Alamo, R.; Fatou, J.G.; Guzman, J. Crystallization of polyformals: 1. Crystallization kinetics of poly(1,3-dioxolane). Polymer **1982**, *23*, 374–378.
34. Clark, E.J.; Hoffman, J.D. Regime III crystallization in polypropylene. Macromolecules **1984**, *17*, 878–885.
35. Janimak, J.J.; Cheng, S.Z.D.; Giusti, P.A.; Hsieh, E.T. Isotacticity effect on crystallization and melting in poly(propylene) fractions. 2. Linear crystal growth rate and morphology study. Macromolecules **1991**, *24*, 2253–2260.
36. Hoffman, J.D.; Miller, R.L. Kinetics of crystallization from the melt and chain folding in polyethylene fractions reviseted: theory and experiments. Polymer **1997**, *38*, 3151–3212.
37. Hoffman, J.D. Regime III crystallization in melt-crystallized polymers: the variable cluster mode of chain folding. Polymer **1983**, *24*, 3–26.
38. Monasse, B.; Haudin, J.M. Growth transition and morphology change in polypropylene. Colloid Polym. Sci. **1985**, *263*, 822–831.
39. Monasse, B.; Haudin, J.M. Effect of random copolymerization on growth transition and morphology change in polypropylene. Colloid Polym. Sci. **1988**, *266*, 679–687.
40. Allen, R.C.; Mandelkern, L. On regimes I and II during polymer crystallization. Polym. Bull. **1987**, *17*, 473–480.

41. Alamo, R.; Fatou, J.G.; Guzman, J. Crystallization of polyformals: 2. Influence of molecular weight and temperature on the morphology and growth rate in poly(1,3-dioxolane). Polymer **1982**, *23*, 379–384.
42. Roitman, D.B.; Marand, H.; Miller, R.L.; Hoffman, J.D. Kinetics of crystallization and morphology of poly(pivalolactone): regime II → III transition and nucleation constants. J. Phys. Chem. **1989**, *93*, 6919–6926.

Received March 7, 2002
Accepted May 27, 2002